Bioorganic & Medicinal Chemistry 22 (2014) 4001–4009

Contents lists available at ScienceDirect

Bioorganic & Medicinal Chemistry

journal homepage: www.elsevier.com/locate/bmc

Discovery of potent and selective spiroindolinone MDM2 inhibitor, RO8994, for cancer therapy

Zhuming Zhang [a,*], Qingjie Ding [a], Jin-Jun Liu [a], Jing Zhang [a], Nan Jiang [a], Xin-Jie Chu [a], David Bartkovitz [a], Kin-Chun Luk [a], Cheryl Janson [b], Christian Tovar [c], Zoran M. Filipovic [c], Brian Higgins [c], Kelli Glenn [d], Kathryn Packman [c], Lyubomir T. Vassilev [c], Bradford Graves [b,*]

[a] Discovery Chemistry, Roche Research Center, Hoffmann-La Roche, Inc., 340 Kingsland Street, Nutley, NJ 07110, United States
[b] Discovery Technologies, Roche Research Center, Hoffmann-La Roche, Inc., 340 Kingsland Street, Nutley, NJ 07110, United States
[c] Discovery Oncology, Roche Research Center, Hoffmann-La Roche, Inc., 340 Kingsland Street, Nutley, NJ 07110, United States
[d] Non-Clinical Development, Roche Research Center, Hoffmann-La Roche, Inc., 340 Kingsland Street, Nutley, NJ 07110, United States

ARTICLE INFO

Article history:
Received 10 April 2014
Revised 23 May 2014
Accepted 30 May 2014
Available online 11 June 2014

Keywords:
MDM2
p53
Protein–protein interaction
Apoptosis
Cancer

ABSTRACT

The field of small-molecule inhibitors of protein–protein interactions is rapidly advancing and the specific area of inhibitors of the p53/MDM2 interaction is a prime example. Several groups have published on this topic and multiple compounds are in various stages of clinical development. Building on the strength of the discovery of RG7112, a Nutlin imidazoline-based compound, and RG7388, a pyrrolidine-based compound, we have developed additional scaffolds that provide opportunities for future development. Here, we report the discovery and optimization of a highly potent and selective series of spiroindolinone small-molecule MDM2 inhibitors, culminating in RO8994.

1. Introduction

Tumor suppressor p53 is a potent transcription factor that plays a central role in guarding the integrity of cell genome.[1–4] In non-stressed cells, p53 is tightly controlled by its master negative regulator MDM2.[5] In about 50% of human cancers, p53 remains wild-type but its function is impaired by other mechanisms, such as overexpression of MDM2.[6–9] Thus, MDM2 has been deemed a valid target for cancer therapy.[10] The early structure of a p53 peptide bound to MDM2 showed that the interactions were mediated by a limited set of amino acids and provided a reasonable expectation that small molecules could successfully interfere with the p53-MDM2 interaction.[11] The discovery of Nutlins verified this approach.[12] An advanced member of the Nutlin family of molecules, **1** (RG7112, Fig. 1), is in clinical evaluation.[13] Internal efforts identified a novel pyrrolidine compound, **2** (RG7388, Fig. 1), which was found to display superior in vitro potency and in vivo efficacy and is progressing in clinical studies.[14] Nevertheless, identification of candidates from distinctive chemical classes may also be desirable to enhance the chances for ultimate success in the clinic.

Since the discovery of Nutlins, several groups have identified additional compound classes and a few have even progressed into clinical development.[15] The most notable one has been a spiroindolinone-3,3′-pyrrolidine MI-219 series reported by Ding et al.[16] Just recently, this group published their latest findings in which the original stereochemistry was found to be unstable and converted over time to a more stable diastereomeric configuration and the most potent compound **3** (MI-888, Fig. 1) was found to achieve tumor regression in mice bearing SJSA-1 xenograft model at a relatively high dose.[17,18] Prior to their work, we also demonstrated that stereochemistry of the pyrrolidine core structure in which the two aryl rings ('A' and 'B') adopt a '*Trans*' orientation as shown in **2** (RG7388, Fig. 1) was important for optimal binding to MDM2.[14] Guided by X-ray co-crystal structures, we further explored the pyrrolidine analogues by combining the key structural elements of **2** (RG7388) and the spiroindolinone core structure of **3** (MI-888).[18,19] Here we report our work leading to the discovery of a potent and highly efficacious compound **4** (RO8994) with promising potential for clinical development (Fig. 1).[19]

* Corresponding authors. Tel.: +1 215 628 7076; fax: +1 215 540 4612 (Z.Z.); tel.: +1 973 680 8039 (B.G.).
E-mail addresses: zzhang85@its.jnj.com (Z. Zhang), bjgraves101@gmail.com (B. Graves).

http://dx.doi.org/10.1016/j.bmc.2014.05.072
0968-0896/

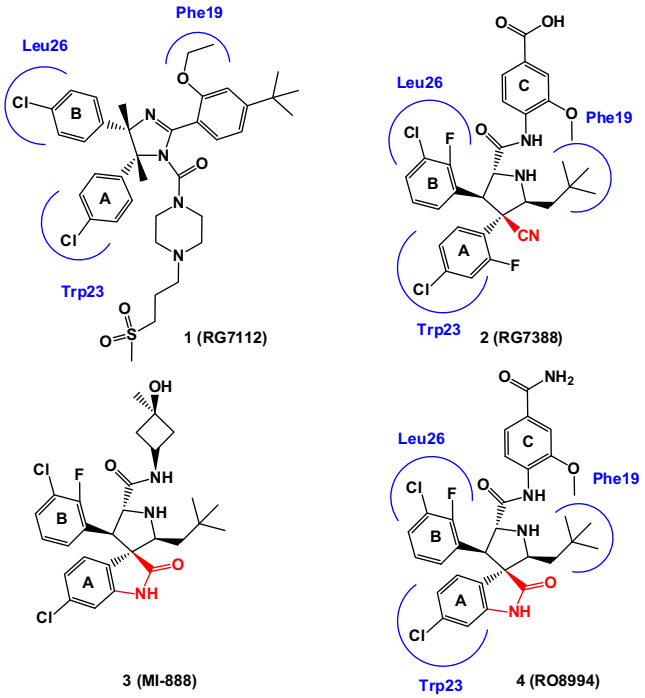

Figure 1. Chemical structures and binding modes of p53–MDM2 inhibitors.

2. Results and discussion

Compared to the identification of Nutlins by high throughput screenings,[12] the discoveries of **2** (RG7388) and **4** (RO8994) were driven by the structure-based *de novo* design and information based approach. Our initial design started with the indolinone compound **5**, which was confirmed to be a validated hit with an IC_{50} of 3.9 μM in a biochemical binding assay (Fig. 2).[20] In the crystal structure, the 6-chlorooxindole ('A') fills the deep, narrow Trp23 pocket. Only the (*S*)-configuration of compound **5** is active, which places the 3-chlorophenyl ('B') in the Leu26 pocket but the binding to Phe19 pocket is suboptimal. As a strategy to optimize compound **5**, rigidifying the structure **6** by cyclizing between the 3,3′ positions with a six- or seven-membered core ring led to the spiroindolinone scaffolds **7** and **9** (Fig. 2 and Scheme 1).[21,22] This was successful in enhancing the binding affinities but unfavorable physicochemical or pharmacological properties rendered these compounds difficult to progress.[23,24] Thus, we shifted our exploration to the five-membered spiroindolinone scaffold **8** (Scheme 1) while simultaneously taking advantage of the knowledge gained from the development of **2** (RG7388, Fig. 1).[14,19]

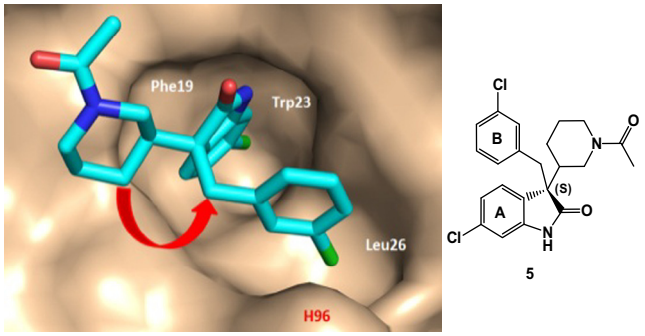

Figure 2. X-ray structure of compound **5** bound to MDM2. The 6-chlorooxindole ring fills the Trp23 pocket. The 3-chloro-phenyl occupies the Leu26 pocket. This structure has been deposited at the PDB (code 4LWT).

Several factors were taken into consideration for our exploration of scaffold **8**. First, the relative spatial orientation of hydrophobic groups in scaffold **8** could be differentiated in relation to scaffold **7** and **9** in terms of binding to MDM2 due to the pseudorotation propensity of pyrrolidine core structure. The five-membered pyrrolidine ring is more flexible than the corresponding six- and seven-membered ring systems and is known to exhibit two predominant puckering modes.[25–27] It was further demonstrated that the stereochemical configuration of the pyrrolidine core structure in which the two aryl rings ('A' and 'B') adopt a '*Trans*' orientation was very important for optimal binding as shown in compound **2** (RG7388, Scheme 2).[14] Second, the use of a substituted *para*-benzoic acid group ('C' in Fig. 1 and Scheme 2) as the R^2 group proved to be critical for RG7388 in lead optimization of the scaffold **10** as it stabilized the molecule metabolically and significantly improved cellular potency/selectivity and PK profiles.[14] Third, the architecture of spiroindolinone-3,3′-pyrrolidine series was initially reported by Ding et al. as shown in compound **12** (MI-219).[16] However, the stereochemical configuration appears to be suboptimal based on the observation by multiple groups that an aromatic ring is preferred in the Leu26 pocket.[24,28] Consistent with these observations, this group recently disclosed their latest findings that original '*Cis*' stereochemistry was found to be unstable and isomerized into a more stable '*Trans*' configuration as shown in **3** (MI-888).[17,29] Compound **3** displayed improved potency and PK over **12** and achieved complete and durable tumor regression in a dose of 100 mg/kg.[18] However, we envisioned the presence of an aromatic ring as R^2 ('C' in Fig. 1 and Scheme 2) would be important and thus expanded our exploration into the analogues **11** (Scheme 2) driven by the impressive in vitro and in vivo potency of **2** (RG7388).[14]

To keep the optimal binding mode to MDM2, the stereochemical configuration of the pyrrolidine in **2** (RG7388) was preserved in analogues **11**. Since the substituted *para*-benzoic acid ('C') group was considered to be a critical element in compound **2**, optimization focused on the phenyl group as the side chain ('C') to diverge from compound **3**. Variations in groups R and R′ were explored for their effects on potency and pharmacological properties. As the R group on the *para*-position points to solvent, different polar or solubilizing groups with electron withdrawing (R = COOH, $CONH_2$) and electron donating properties (R = OCH_2CH_2OH) were selected and combined with small R′ groups at the 2- or 3-position to minimize metabolic liability, enhance cellular potency, and maximize PK parameters. The impact of a fluorine substituent (R^3 = F) at the 4-, 5- or 7-position of the 6-chlorooxindole on potency was also examined.

The synthesis of analogs in scaffold **8** is outlined in Scheme 3.[29] The preparation of the desired stereochemical configuration in the pyrrolidine core structure **8** was problematic prior to our work. AgF mediated 1,3-dipolar cycloaddition reaction of 3-benzylidene oxindole **13** with imine **14** led mostly to spiroindolinone **15** with predominant '*Cis*' configuration between the aryl rings ('A' and 'B') likely due to the pre-established '*Cis*' or (*E*)-configuration in **13**.[30–32] Other diastereomers were also observed but only trace amounts of the desired spiroindolinone **16** with '*Trans*' configuration was observed. By contrast, the '*Trans*' configuration was generated for the pyrrolidine compound **2** (RG7388) series under similar reaction conditions as the results of the predominant '*Trans*' configuration in (Z)-α-cyanostilbene.[14] The formation of spiroindoline **15** is clearly kinetically favored.[17,29,33] After some explorations, it was found that treatment of **15** with DBU under heating conditions could afford key intermediate **16**. The isomerization from **15** to **16** involves the inversion of two stereocenters and occurs most likely via a retro-Mannich reaction followed by a ring-closure

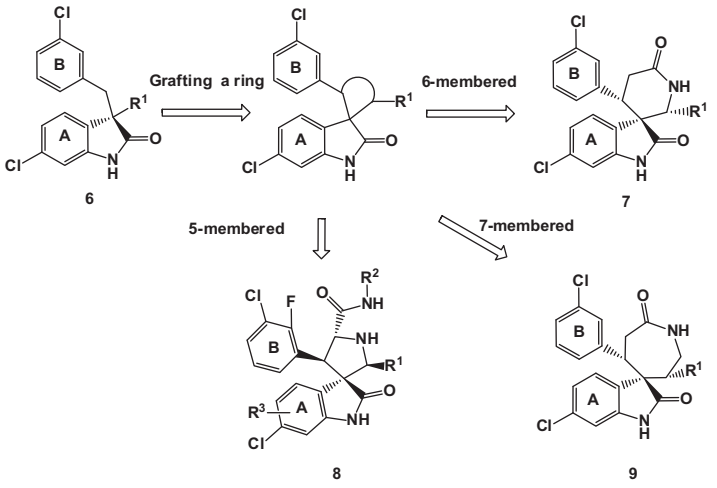

Scheme 1. Variations of spiroindolinone scaffolds as p53–MDM2 inhibitors.

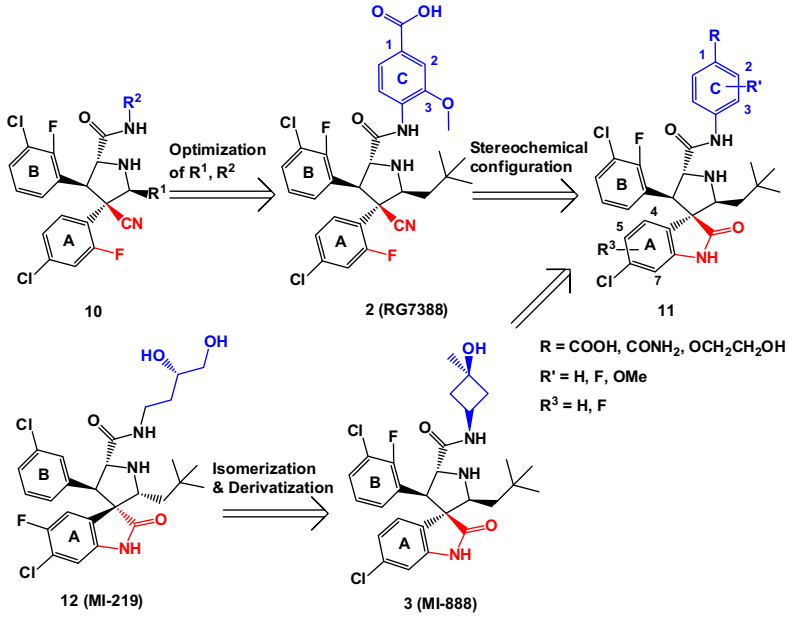

Scheme 2. The evolution of MDM2 inhibitors from RG7388, **3** (MI-888) to analogues **11**.

Mannich reaction.[29] Our studies indicated that the stereochemical configuration in compound **16** could be thermodynamically preferred albeit kinetically less favorable. The analogs in scaffold **8** were synthesized initially as a racemic mixture from which the two chiral enantiomers can be separated by chiral SFC. The preparation of analogues in scaffold **8** was later optimized by internal process research and the method can be amenable to the production of multihundred gram scale.[29]

The biochemical binding and cellular antiproliferative activity of analogs **4** and **18**–**27** are summarized in Table 1. In the biochemical HTRF binding assay, all are highly active with IC_{50} <20 nM (Fig. 3 and Table 1) and compare favorably with **2** (RG7388). Compound **18** (IC_{50} = 4 nM) is >900-fold more potent than its enantiomer (**18′**, IC_{50} = 3741 nM) (SI Table S1). The absolute stereochemical configuration and binding mode of the more active enantiomer was confirmed by determination of the crystal structure of compound **20** bound to MDM2 (Fig. 4). The 6-chlorooxindole occupies the Trp23 pocket with the NH forming a hydrogen bond with protein backbone. The neopentyl group is located in the Phe19 pocket. The 3-chloro-2-fluorophenyl ring is buried in the Leu26 pocket, forming a π–π stacking interaction with the His96 residue on MDM2. The pyrrolidine carbonyl forms a hydrogen bond with NH of the His96 side chain.

By inspection of available co-crystal structures, it appears that an aromatic moiety is favored over an aliphatic group in the Leu26 pocket of MDM2 in spite of pseudosymmetric spatial relationship of Leu26 and Phe19 pockets.[24,28] The presence of His96 residue in the Leu26 pocket is an important structural feature for the differentiation of these two pockets in terms of designing novel MDM2 inhibitors (Fig. 4). The interaction with His96 residue could be a key factor for the high MDM2 binding affinities of these compounds and also explain the lack of binding to MDMX.[24,28] The mismatch of aromatic and aliphatic elements in the Leu26 and Phe19 pockets also appears to be a common motif between non-peptide small molecules and peptide inhibitors. Further exploration and elaboration in these areas will have important implications for the design of MDMX or MDM2/MDMX dual inhibitors.[24,34,35]

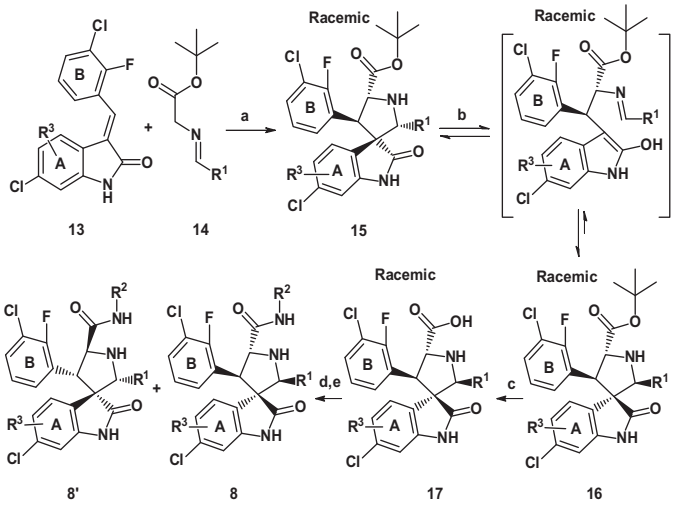

Scheme 3. The racemic synthesis of designed analogues in spiroindolinone scaffold **8**. Reagents and conditions: (a) AgF, NEt_3, DCM, rt; (b) DBU, *t*BuOH, reflux; (c) TFA, DCM, rt; (d) NH_2R^2, $Ph_2C(=O)Cl$, $^iPr_2NEt$, DCM, rt; (e) chiral SFC separation **11**.

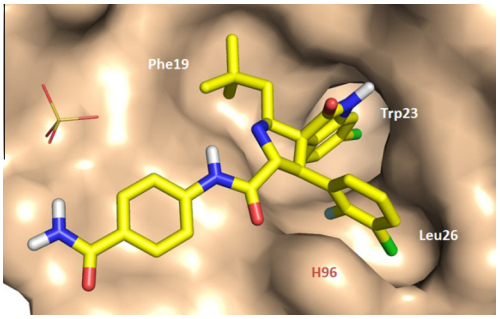

Figure 4. X-ray structure of spiroindolinone **20** bound to MDM2. This structure has been deposited at the PDB (code 4LWU).

In the cellular proliferation (MTT) assays, compounds **4** and **18**–**24** displayed potent anti-proliferative activities with average MTT IC_{50} ranging from 0.01 to 0.19 μM against three wild-type p53 human cancer cell lines (SJSA1, RKO, HCT116). Selectivity, defined as the ratio of average IC_{50} values derived from mutant (SW480 & MDA-MB-435) and wild-type p53 cell lines, ranged from 51- to 882-fold (Table 1). Cellular potency and selectivity of the better compounds track well with those for **2** (RG7388). In spite of the

Table 1
In vitro activity of spiroindolinone analogues **18**–**27**, **4** and **2** (RG7388) in HTRF binding assays and MTT proliferation assays with human cancer cell lines[a]

Compound	**18**	**19**	**20**	**21**	**22**	**4**	**23**	**24**	**25**	**26**	**27**	**2** (RG7388)
HTRF IC_{50} (μM)	0.004	0.005	0.005	0.005	0.007	0.005	0.008	0.005	0.006	0.006	0.018	0.006
MTT IC_{50}[b] (μM)	0.15	0.01	0.09	0.06	0.13	0.02	0.19	0.01	0.09	0.25	0.69	0.03
Selectivity[c]	89	882	150	82	67	312	57	782	132	51	12	344

[a] IC_{50} was determined by one experiment performed in duplicate.
[b] Average IC_{50} of three wt-p53 cancer cell lines (SJSA1, RKO, HCT116).
[c] Ratio of average IC_{50} of two mutant p53 cell lines (SW480, MDA-MB-435) and average IC_{50} of three wild-type p53 cell lines (as above).

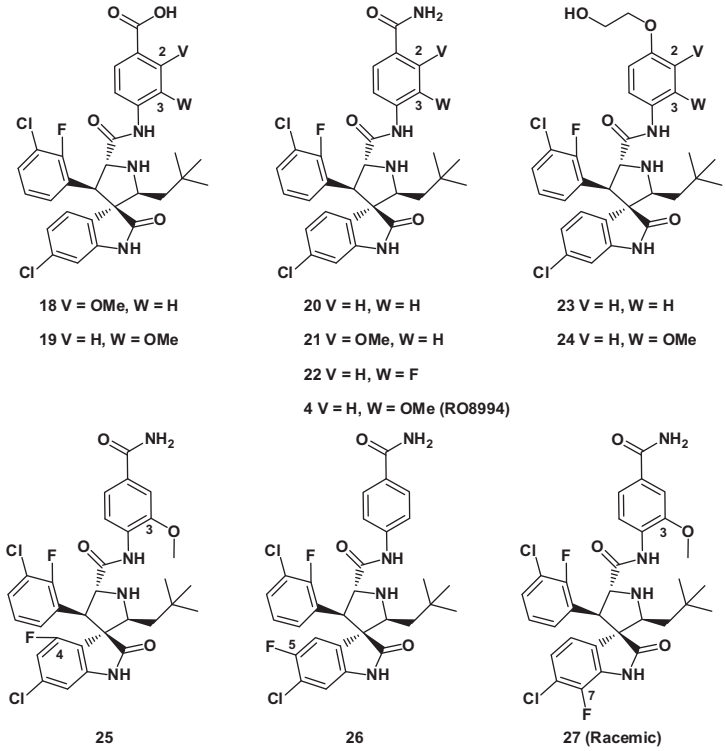

Figure 3. The chemical structures of spiroindolinone analogues in scaffold **8**.

Table 2
The human liver microsomal stability and mean PK parameters of compounds **19**, **20**, **22**, **4**, **24**, **26** and RG7388 in C57 male mice by single oral and iv dosing

Compound	**19**	**20**	**22**	**4**	**24**	**26**	**2** (RG7388)
HLM_CL[a] (mL/min/kg)	12.0	7.5	7.4	7.5	5.1[c]	9.3	4.3
PO Dose (mg/kg)	25	50	50	25	25	50	50
PO AUC/PO dose (μg*h/mL/mg/kg)	0.1	3.0	3.4	3.7	1.4	2.6	1.3
PO C_{max} (μg/mL)	0.8	8.3	13.1	5.8	4.3	8.7	9.9
iv dose (mg/kg)	5	5	5	0.64	5	5	5
CL (mL/min/kg)	34.6	3.5	3.4	5.8	6.7	2.6	10.3
$T_{1/2}$ (h)	11.1	10.4	15.3	7.1	6.6	8.8	1.6
F[b] (%)	21	63	75	92	55	45	80

[a] For HLM_CL: low clearance < 6.5, 6.5 < medium clearance < 35, high clearance > 35.
[b] Oral bioavailability.
[c] In vitro human hepatocyte clearance rat.

difference in polar groups at the *para* position, compounds **19**, **4**, and **24** showed excellent cellular potency and selectivity that are at least as good as those observed for **2**. All three compounds possess a 3-methoxy group on the phenyl ring (as does **2**). Compounds with no methoxy group (**20** and **23**) or with a 2-methoxy (**18** and **21**) were clearly less potent and less selective, recapitulating the preference for the 3-methoxy substitution observed with the optimization resulting in **2**.[14] Similarly, 3-fluoro (compound **22**) was not as active or selective. Compound **19** displayed a cellular MTT IC_{50} of 0.01 μM and a selectivity of 882, indicating that replacement of 4-chloro-2-fluorophenyl in **2** with 6-chlorooxindole led to enhanced cellular potency and selectivity presumably due to the formation of hydrogen bond between 6-chlorooxindole and protein backbone. Mono-fluoro substitution on the 4- or 5-position of 6-chlorooxindole led to a loss in cellular potency/selectivity (compare compounds **25**, **26** to corresponding **4**, **20**). Substitution with fluorine at the 7-position is clearly detrimental and led to a substantial loss in cellular potency/selectivity (compare **27** to **4**).

Compounds **19**, **20**, **22**, **4**, **24**, **26** were selected for in vivo pharmacokinetic (PK) evaluation based on their parameters in human liver microsomal stability or cellular potency/selectivity (Table 2). Compound **19** showed suboptimal oral bioavailability and a high clearance rate despite its impressive cellular potency and identical side chain with **2**. By contrast, compounds **20**, **22**, **4** showed excellent PK properties, with dose-normalized exposures that are ~2.5-fold higher than **2**. It is noteworthy that the only structural difference between **4** and **19** is the terminal carboxamide versus carboxylic acid. Thus, in spite of the many parallel trends between this spiroindolinone series **8** and the RG7388 series **10**, there are subtle differences. Within the carboxamide series in **11**, the presence of 3-methoxy in compound **4** led to not only higher cellular potency and selectivity (as mentioned above) but also a higher oral bioavailability over compound **20**. This trend was also observed in optimization of the RG7388 series. However, despite a similar clearance rate in in vivo PK studies, the oral bioavailability of **24** is much lower than that of **4**. The discrepancy could be explained by their difference in physicochemical properties such as permeability (data not shown). The 5-position of 6-chlorooxindole was considered to be a potential metabolic hotspot for oxidative

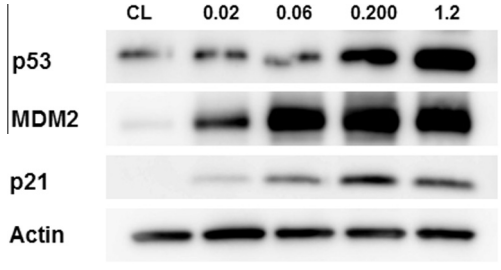

Figure 5. Weston blot analysis of p53 activation induced by compound **4** (RO8994) in SJSA osteosarcoma tumor tissue.

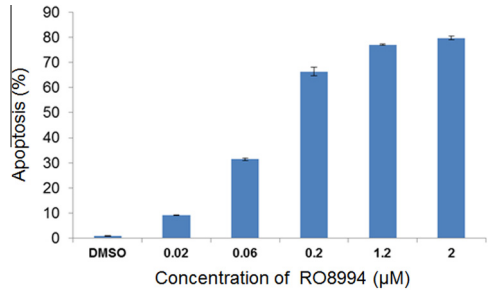

Figure 6. Apoptosis in SJSA cells treated with compound **4**. Cells were incubated for 48 h.

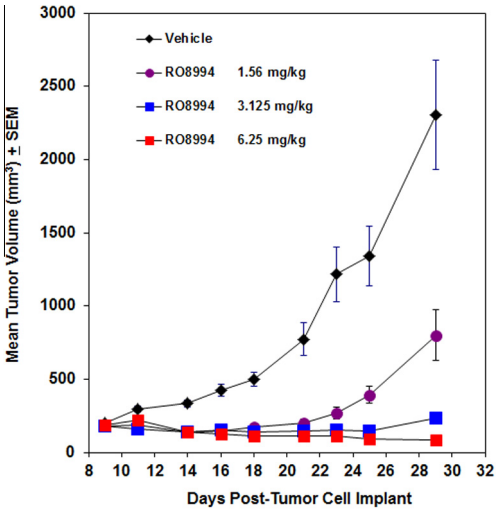

Figure 7. The oral in vivo efficacy profile of **4** (RO8994) in the SJSA-1 human osteosarcoma xenograft model in nude mice. Tumor growth inhibition was observed at 1.56 mg/kg qd and tumor regression was observed at 6.25 mg/kg qd.

hydroxylation. It was hypothesized that blocking this site could potentially improve metabolic liability. However, 5-fluoro substitution offers no noticeable improvement in PK parameters (compare **26** to **20**). Thus, the data so far suggest that the 6-chlorooxindole group is optimal for these analogs in scaffold **8.**

While not the most potent or selective in the series, compound **4** was chosen for further study based on the balance of its excellent in vitro activities and in vivo pharmacological profile. From in vitro mechanistic studies, compound **4** induced dose-dependent up-regulation of p53 target genes and apoptosis in wild-type p53 cancer cells, consistent with its non-genotoxic mechanism of p53 activation (Figs. 5 and 6, respectively).[10] Compound **4** also displayed remarkable tumor growth inhibition in the wild-type p53, MDM2-amplified SJSA-1 osteosarcoma tumor xenograft

model (Fig. 7)—exhibiting significant (>60%) tumor growth inhibition at the low dose of 1.56 mg/kg, tumor stasis at 3.125 mg/kg and regression at 6.25 mg/kg. This would appear to be at least as good as the efficacy results with **2** (RG7388) and significantly more efficacious than **3** (MI-888).[14,18]

3. Conclusion

In summary, our investigation of 5-membered spiroindolinones **8** led to the identification of a highly potent and selective p53-MDM2 inhibitor **4** (RO8994). The synthesis of compound **4** has been optimized for large scale and the compound has also demonstrated acceptable toxicity profiles in both rodent and non-rodent dose range finding studies (data not shown).[29] Like **2** (RG7388), compound **4** (RO8994) represents a new generation of p53–MDM2 antagonists with marked improvement in both in vitro and in vivo pharmacological properties for potential clinical development. The further exploration of additional chemical series on the basis of RO8994 has led to the identification of two new potent MDM2 RO5353 and RO2468.[36] Our studies also highlighted a subtle difference of MDM2 inhibitors in mimicking Leu26 and Phe19 residue of p53. The mismatch of Leu26 and Phe19 binding groups between non-peptide small molecules and peptide inhibitors appears to be a common motif and further exploration of structural difference would have implications in design of MDMX or dual MDM2/MDMX non-peptide small-molecule inhibitors.

4. Experimental section

4.1. General chemistry

All commercial reagents and anhydrous solvents were purchased and used without further purification, unless otherwise specified. Mass samples were analyzed on a MicroMass ZQ, ZMD, Quattro LC, or Quattro II mass spectrometer operated in a single MS mode with electrospray ionization. High resolution mass spectra (HRMS) were measured on a Bruker Daltonics APEXII 3 Tesla Fourier transform mass spectrometer. ^{1}H NMR spectra (δ, ppm) were recorded using either a Bruker Avance 400 (400 MHz) or a Bruker Avance II-300 (300 MHz) instrument. ^{1}H and ^{13}C NMR chemical shifts are reported in parts per million (δ) relative to the ^{1}H and ^{13}C signals in the solvent ($CDCl_3$: δ 7.26, 77.16 ppm; DMSO-d_6: δ 2.50, 39.52 ppm). Column chromatography was performed using an ISCO Combiflash or glass column packed with Merck silica gel 60 (0.040–0.063 mm). All compounds for biological assays were >95% pure by HPLC (Column: Zorbax SB-CN, 3.5 μm, 120 A, 150 mm × 4.6 mm i.d.; mobile phases: 35% Acetonitrile and 65% water plus 0.2% H_3PO_4 over 30 min; column temperature: room temperature; detector setting: UV at 220 nm; flow rate: 1.0 mL/min).

Synthesis of racemic **17** from intermediates **13** and **14** (Scheme 3) either has been reported recently[29] or described in SI section (R^3 = H, F; R^1 = $CH_2C(CH_3)_3$).

4.2. General procedures for preparation of compounds 18, 18′ and 19 from racemic 17 (R^3 = H, R^1 = $CH_2C(CH_3)_3$)

Step (*A*): To a solution of racemic (2′*S*,3′*R*,4′*S*,5′*R*)-6-chloro-4′-(3-chloro-2-fluoro-phenyl)-2′-(2,2-dimethyl-propyl)-2-oxo-1,2-dihydro-spiro[indole-3,3′-pyrrolidine]-5′-carboxylic acid trifluoroacetic acid salt **17** (R^3 = H, R^1 = $CH_2C(CH_3)_3$, Ref. 29) (0.2 g, 0.36 mmol) in dichloromethane (10 mL) was added diisopropylethylamine (0.18 g, 1.4 mmol), diphenylphosphinic chloride (Aldrich) (0.25 g, 1.1 mmol), respectively. The mixture was stirred at room temperature for 0.5 h, then methyl 4-amino-2-methoxybenzoate (Acros) (0.077 g, 0.43 mmol) or methyl 4-amino-3-methoxy-benzoate (Ark Pharm) (0.16 g, 0.9 mmol) was added. The reaction mixture was stirred at room temperature for 20 h. The mixture was concentrated. The residue was partitioned between ethyl acetate and water. The organic layer was separated, washed with water, brine, dried over Na_2SO_4, then concentrated. The residue was purified by chromatography (3–20% of EtOAc in CH_2Cl_2) to give a white solid (yield 0.12 g, 54%).

Step (*B*): To a solution of the white solid from Step (A) (0.1 g, 0.16 mmol) in tetrahydrofuran (20 mL) was added an aqueous solution (1 N) of NaOH (8 mL, 8 mmol) and methanol (8 mL). The reaction mixture was heated at 80 °C for 1 h, and then cooled to room temperature. The 'pH' of the mixture was adjusted to 5–6 by aqueous HCl solution, then concentrated to a small volume. The residue was partitioned between ethyl acetate and water. The organic layer was separated, and the aqueous layer was extracted with ethyl acetate twice. The combined organic extract was washed with water, brine, dried over $MgSO_4$, and concentrated to give the racemic product as an off white solid (75 mg, 77%).

Step (*C*): The racemic product from Step (B) was separated by chiral SFC chromatography (prep OJ, or AD, or OD, 35 °C at 100 bar, eluting with 20–40% methanol in carbon dioxide) to provide pure two enantiomers (>95% ee).

4.3. Chiral 4-{[(2′*S*,3′*R*,4′*S*,5′*R*)-6-chloro-4′-(3-chloro-2-fluoro-phenyl)-2′-(2,2-dimethyl-propyl)-2-oxo-1,2-dihydro-spiro[indole-3,3′-pyrrolidine]-5′-carbonyl]-amino}-2-methoxy-benzoic acid (18)

A light yellow solid (40 mg, 36%). ^{1}H NMR (300 MHz, DMSO-d_6) δ 10.46 (s, 1H), 10.27 (s, 1H), 7.69 (d, J = 8.53 Hz, 1H), 7.63 (d, J = 8.03 Hz, 1H), 7.51–7.60 (m, 2H), 7.36 (t, J = 7.09 Hz, 1H), 7.10–7.20 (m, 1H), 7.04 (dd, J = 1.81, 8.00 Hz, 1H), 6.97 (d, J = 8.45 Hz, 1H), 6.68 (d, J = 1.81 Hz, 1H), 4.72 (d, J = 9.36 Hz, 1H), 4.56 (d, J = 9.36 Hz, 1H), 3.84 (d, J = 9.36 Hz, 1H), 3.75 (s, 3H), 1.25 (dd, J = 9.51, 13.74 Hz, 1H), 0.82 (s, 9H), 0.72–0.78 (m, 1H) ppm; ^{13}C NMR (101 MHz, DMSO-d_6) δ 177.0, 172.1, 166.4, 159.6, 156.8, 154.3, 143.4, 142.9, 132.4, 129.2, 128.3, 126.0, 125.9, 125.0, 124.9, 121.4, 119.4, 119.2, 115.1, 110.0, 109.3, 102.2, 65.5, 64.8, 64.5, 55.6, 47.9, 43.3, 30.0, 29.7 ppm; HRMS (ES^+) m/z calcd for $C_{31}H_{30}Cl_2FN_3O_5$+H [$(M+H)^+$]: 614.1620, found: 614.1617.

4.4. Chiral 4-{[(2′*R*,3′*S*,4′*R*,5′*S*)-6-chloro-4′-(3-chloro-2-fluoro-phenyl)-2′-(2,2-dimethyl-propyl)-2-oxo-1,2-dihydro-spiro[indole-3,3′-pyrrolidine]-5′-carbonyl]-amino}-2-methoxy-benzoic acid (18′)

A light yellow solid (39 mg, 35%). ^{1}H NMR (300 MHz, DMSO-d_6) δ 10.49 (s, 1H), 10.30 (s, 1H), 7.72 (d, J = 8.53 Hz, 1H), 7.65 (d, J = 8.03 Hz, 1H), 7.56–7.63 (m, 2H), 7.39 (t, J = 7.09 Hz, 1H), 7.18 (t, J = 7.91 Hz, 1H), 7.07 (dd, J = 1.76, 8.03 Hz, 1H), 7.01 (dd, J = 1.51, 8.53 Hz, 1H), 6.71 (d, J = 1.76 Hz, 1H), 4.75 (d, J = 9.36 Hz, 1H), 4.60 (d, J = 9.36 Hz, 1H), 3.87 (d, J = 9.36 Hz, 1H), 3.79 (s, 3H), 1.29 (dd, J = 9.66, 13.74 Hz, 1H), 0.85 (s, 9H), 0.79 (d, J = 13.74 Hz, 1H) ppm; ^{13}C NMR (101 MHz, DMSO-d_6) δ 177.0, 172.1, 166.4, 159.6, 156.8, 154.3, 143.4, 142.9, 132.4, 129.2, 128.3, 126.1, 125.1, 124.9, 121.4, 119.4, 119.2, 115.1, 110.0, 109.3, 102.2, 65.5, 64.9, 64.6, 55.6, 47.9, 43.3, 30.0, 29.7 ppm; HRMS (ES^+) m/z calcd for $C_{31}H_{30}Cl_2FN_3O_5$+H [$(M+H)^+$]: 614.1620, found: 614.1614.

4.5. Chiral 4-{[(2′*S*,3′*R*,4′*S*,5′*R*)-6-chloro-4′-(3-chloro-2-fluoro-phenyl)-2′-(2,2-dimethyl-propyl)-2-oxo-1,2-dihydro-spiro[indole-3,3′-pyrrolidine]-5′-carbonyl]-amino}-3-methoxy-benzoic acid (19)

A white solid (57 mg, 37%). ^{1}H NMR (400 MHz, DMSO-d_6) δ 10.79 (s, 1H), 10.56 (br s, 1H), 8.43 (d, J = 8.53 Hz, 1H), 7.72 (d, J = 8.03 Hz, 1H), 7.56–7.67 (m, 3H), 7.38 (t, J = 7.15 Hz, 1H), 7.18

(t, J = 7.78 Hz, 1H), 7.03 (d, J = 8.03 Hz, 1H), 6.72 (s, 1H), 4.69 (d, J = 9.29 Hz, 1H), 4.50 (d, J = 9.29 Hz, 1H), 3.93 (s, 3H), 3.87 (d, J = 9.85 Hz, 1H), 1.32 (dd, J = 9.85, 13.49 Hz, 1H), 0.93 (s, 9H), 0.79 (d, J = 13.49 Hz, 1H) ppm; ^{13}C NMR (101 MHz, DMSO-d_6) δ 176.9, 172.1, 167.0, 156.8, 154.3, 147.5, 143.4, 132.4, 131.4, 129.0, 128.4, 126.6, 125.7, 125.6, 125.3, 124.8, 122.7, 121.4, 119.2, 117.0, 110.9, 109.3, 65.9, 65.0, 55.7, 48.8, 42.7, 30.0, 29.6 ppm; ^{13}C NMR (101 MHz, DMSO-d_6) δ 176.9, 172.1, 167.0, 156.8, 154.3, 147.5, 143.4, 132.4, 131.4, 129.0, 128.4, 126.7, 126.6, 125.7, 125.6, 125.3, 124.8, 124.8, 122.7, 121.4, 119.3, 119.1, 117.0, 110.9, 109.3, 65.9, 65.1, 65.0, 55.7, 48.8, 42.7, 30.0, 29.6 ppm; HRMS (ES$^+$) m/z calcd for $C_{31}H_{30}Cl_2FN_3O_5$+H [(M+H)$^+$]: 614.1619, found: 614.1606. $[\alpha]_D^{20}$ = −54.0° (c 0.08, MeOH).

4.6. General procedures for preparation of compounds 20–22, 4 from racemic 17 (R^3 = H, R^1 = $CH_2C(CH_3)_3$)

Step (*A*): In a manner similar to the method described in general procedure (A) for compound **18**, **18′** and **19**, racemic (2′*S*,3′*R*,4′*S*,5′*R*)-6-chloro-4′-(3-chloro-2-fluoro-phenyl)-2′-(2,2-dimethyl-propyl)-2-oxo-1,2-dihydro-spiro[indole-3,3′-pyrrolidine]-5′-carboxylic acid trifluoroacetic acid salt **17** (R^3 = H, R^1 = $CH_2C(CH_3)_3$) (2.94 g, 5.07 mmol) was reacted with diisopropylethylamine (5.25 g, 40.6 mmol), diphenylphosphinic chloride (4.8 g, 20.3 mmol), then corresponding optionally substituted 4-aminobenzonitrile (2.4 g, 20.3 mmol) to give the coupled product as an off white foam (Yield 1 g, 34%).

Step (*B*): To a solution of the above coupled product from (A) (0.35 g, 0.62 mmol) in DMSO (7 mL) at 0 °C was added an aqueous solution (30% Aldrich) of H_2O_2 (1.05 g, 9.3 mmol), followed by the addition of aqueous solution (1 N) of NaOH (3 mL, 3 mmol) dropwise. The reaction mixture was stirred at 0 °C for 1 h. The mixture was partitioned between ethyl acetate and saturated aqueous Na_2SO_3 solution. The organic layer was separated, washed with water, brine, dried over $MgSO_4$, and concentrated. The residue was purified by chromatography (50–100% EtOAc in DCM) to give the racemic product as a white solid (yield 0.26 g, 72%).

Step (*C*): The above racemic product from (B) was separated by chiral SFC chromatography (prep OJ, or AD, or OD, 35 °C at 100 bar, eluting with 20–40% methanol in carbon dioxide) to provide pure two enantiomers (>95% ee).

4.7. Chiral (2′*S*,3′R,4′*S*,5′*R*)-6-chloro-4′-(3-chloro-2-fluoro-phenyl)-2′-(2,2-dimethyl-propyl)-2-oxo-1,2-dihydro-spiro[indole-3,3′-pyrrolidine]-5′-carboxylic acid (4-carbamoyl-phenyl)-amide (20)

A white solid (0.134 g, 25%). ^{1}H NMR (400 MHz, DMSO-d_6) δ 10.51 (s, 1H), 10.26 (s, 1H), 7.91 (br s, 1H), 7.90 (d, J = 8.78 Hz, 2H), 7.65 (d, J = 8.78 Hz, 2H), 7.57–7.61 (m, 2H), 7.35–7.40 (m, 1H), 7.29 (br s, 1H), 7.17 (t, J = 8.03 Hz, 1H), 7.07 (dd, J = 1.89, 8.03 Hz, 1H), 6.72 (d, J = 1.89 Hz, 1H), 4.74 (t, J = 8.41 Hz, 1H), 4.58 (d, J = 9.72 Hz, 1H), 3.89 (t, J = 8.41 Hz, 1H), 3.56 (br s, 1H), 1.30 (dd, J = 9.72, 13.74 Hz, 1H), 0.86 (s, 9H), 0.80 (d, J = 13.74 Hz, 1H) ppm; ^{13}C NMR (101 MHz, DMSO-d_6) δ 177.0, 171.9, 167.3, 156.8, 154.3, 143.4, 140.8, 132.5, 129.1, 128.6, 128.2, 126.2, 126.0, 125.9, 125.1, 124.9, 121.4, 119.4, 119.2, 118.0, 109.3, 65.5, 64.9, 64.6, 48.1, 43.2, 30.0, 29.7 ppm; HRMS (ES$^+$) m/z calcd for $C_{30}H_{29}Cl_2FN_4O_3$+H [(M+H)$^+$]: 583.1674, found: 583.1674. $[\alpha]_D^{20}$ = −21.8° (c 0.11, MeOH).

4.8. Chiral (2′*S*,3′*R*,4′*S*,5′*R*)-6-chloro-4′-(3-chloro-2-fluoro-phenyl)-2′-(2,2-dimethyl-propyl)-2-oxo-1,2-dihydro-spiro[indole-3,3′-pyrrolidine]-5′-carboxylic acid (4-carbamoyl-3-methoxy-phenyl)-amide (21)

An off white solid (10 mg, 14%). ^{1}H NMR (300 MHz, DMSO-d_6) δ 10.47 (s, 1H), 10.27 (s, 1H), 7.85 (d, J = 8.76 Hz, 1H), 7.62–7.66 (m, 2H), 7.55 (br s, 2H), 7.45 (br s, 1H), 7.38 (t, J = 7.09 Hz, 1H), 7.16 (t, J = 8.00 Hz, 1H), 7.06 (dd, J = 1.66, 8.15 Hz, 1H), 7.00 (d, J = 8.76 Hz, 1H), 6.69 (d, J = 1.66 Hz, 1H), 4.69–4.78 (m, 1H), 4.57 (d, J = 9.66 Hz, 1H), 3.85 (s, 3H), 3.81–3.90 (m, 1H), 3.46–3.57 (m, 1H), 1.22–1.31 (m, 1H), 0.84 (s, 9H), 0.79 (d, J = 13.89 Hz, 1H) ppm; HRMS (ES$^+$) m/z calcd for $C_{31}H_{30}Cl_2FN_4O_4$+H [(M+H)$^+$]: 613.1779, found: 613.1779.

4.9. Chiral (2′*S*,3′*R*,4′*S*,5′*R*)-6-chloro-4′-(3-chloro-2-fluoro-phenyl)-2′-(2,2-dimethyl-propyl)-2-oxo-1,2-dihydro-spiro[indole-3,3′-pyrrolidine]-5′-carboxylic acid (4-cyano-2-fluoro-phenyl)-amide (22)

An off white solid (49 mg, 33%). ^{1}H NMR (400 MHz, DMSO-d_6) δ 10.54 (d, J = 2.26 Hz, 1H), 10.47 (s, 1H), 8.38 (t, J = 8.16 Hz, 1H), 7.97 (br s, 1H), 7.80 (dd, J = 1.63, 11.92 Hz, 1H), 7.73 (d, J = 8.53 Hz, 1H), 7.70 (d, J = 8.03 Hz, 1H), 7.60 (t, J = 7.28 Hz, 1H), 7.43 (br s, 1H), 7.35–7.41 (m, 1H), 7.17 (t, J = 8.03 Hz, 1H), 7.04 (dd, J = 1.76, 8.03 Hz, 1H), 6.68 (d, J = 1.76 Hz, 1H), 4.68–4.74 (m, 1H), 4.53 (d, J = 9.60 Hz, 1H), 3.87–3.95 (m, 1H), 3.72–3.81 (m, 1H), 1.29 (dd, J = 9.60, 13.87 Hz, 1H), 0.86 (s, 9H), 0.75 (d, J = 13.87 Hz, 1H) ppm; HRMS (ES$^+$) m/z calcd for $C_{30}H_{28}Cl_2F_2N_4O_3$+H [(M+H)$^+$]: 601.1580, found: 601.1575.

4.10. Chiral (2′*S*,3′*R*,4′*S*,5′*R*)-6-chloro-4′-(3-chloro-2-fluoro-phenyl)-2′-(2,2-dimethyl-propyl)-2-oxo-1,2-dihydro-spiro[indole-3,3′-pyrrolidine]-5′-carboxylic acid (4-carbamoyl-2-methoxy-phenyl-phenyl)-amide (4)

An off white solid (68 mg, 31%). ^{1}H NMR (300 MHz, DMSO-d_6) δ 10.73 (br s, 1H), 10.50 (br s, 1H), 8.37 (d, J = 8.28 Hz, 1H), 7.96 (br s, 1H), 7.74 (d, J = 7.78 Hz, 1H), 7.58–7.67 (m, 2H), 7.54 (d, J = 8.28 Hz, 1H), 7.35–7.43 (m, 1H), 7.32 (br s, 1H), 7.19 (t, J = 7.78 Hz, 1H), 7.01–7.07 (m, 1H), 6.71 (br s, 1H), 4.65–4.73 (m, 1H), 4.50 (d, J = 9.29 Hz, 1H), 3.93 (s, 3H), 3.86 (d, J = 9.80 Hz, 1H), 3.74 (t, J = 10.54 Hz, 1H), 1.32 (dd, J = 9.80, 13.60 Hz, 1H), 1.28–1.37 (m, 1H), 0.94 (br s, 9H), 0.79 (d, J = 13.60 Hz, 1H) ppm; ^{13}C NMR (101 MHz, DMSO-d_6) δ 176.9, 171.9, 167.3, 156.8, 154.3, 147.4, 143.4, 132.4, 129.9, 129.0, 128.4, 126.7, 126.6, 125.8, 125.3, 124.8, 121.4, 120.4, 119.3, 119.1, 116.8, 109.8, 109.2, 65.9, 65.0, 55.7, 48.8, 42.7, 30.0, 29.6 ppm; HRMS (ES$^+$) m/z calcd for $C_{31}H_{31}Cl_2FN_4O_4$+H [(M+H)$^+$]: 613.1779, found: 613.1779. $[\alpha]_D^{20}$ = −45.1° (c 0.07, MeOH).

4.11. General procedures for preparation of compounds 23, 24 from racemic 17 (R^3 = H, R^1 = $CH_2C(CH_3)_3$)

Step (*A*): To a solution of racemic (2′*S*,3′*R*,4′*S*,5′*R*)-6-chloro-4′-(3-chloro-2-fluoro-phenyl)-2′-(2,2-dimethyl-propyl)-2-oxo-1,2-dihydro-spiro[indole-3,3′-pyrrolidine]-5′-carboxylic acid trifluoroacetic acid salt **17** (R^3 = H, R^1 = $CH_2C(CH_3)_3$) (0.4 g, 0.69 mmol) in dichloromethane (9 mL) was added diisopropylethylamine (0.46 g, 3.6 mmol), diphenylphosphinic chloride (Aldrich) (0.34 g, 1.42 mmol) respectively. The mixture was stirred at room temperature for 8 min, then 2-(4-aminophenoxy)ethanol (0.16 g, 1.1 mmol) or 4-[2-(*tert*-butyl-dimethyl-silanyloxy)-ethoxy]-2-methoxy-phenylamine (prepared in SI section) (0.32 g, 1.1 mmol) was added. The reaction mixture was stirred at room temperature for 72 h. The mixture was concentrated. The residue was dissolved into tetrahydrofuran (9 mL), and an aqueous solution (1 N) of HCl (1 mL) was added. The reaction mixture was stirred at room temperature for 2 h, then concentrated. The residue was partitioned between ethyl acetate and aqueous saturated $NaHCO_3$ solution. The organic layer was separated, and aqueous layer was extracted with ethyl acetate twice. The combined organic extract was washed with water, brine, dried over Na_2SO_4, then concentrated.

The residue was purified by chromatography (0–50% of EtOAc in CH_2Cl_2) to give the racemic product as an off white solid (0.18 g, 41%).

Step (*B*): The above racemic product from (A) was separated by chiral SFC chromatography (prep OJ, or AD, or OD, 35 °C at 100 bar, eluting with 20–40% methanol in carbon dioxide) to provide pure two enantiomers (>95% ee).

4.12. Chiral (2′*S*,3′*R*,4′*S*,5′*R*)-6-chloro-4′-(3-chloro-2-fluoro-phenyl)-2′-(2,2-dimethyl-propyl)-2-oxo-1,2-dihydro-spiro[indole-3,3′-pyrrolidine]-5′-carboxylic acid [4-(2-hydroxy-ethoxy)-phenyl]-amide (23)

An off white solid (38 mg, 41%). ^{1}H NMR (400 MHz, DMSO-d_6) δ 10.47 (s, 1H), 9.92 (s, 1H), 7.63 (d, J = 8.03 Hz, 1H), 7.58 (t, J = 6.90 Hz, 1H), 7.46 (d, J = 9.04 Hz, 2H), 7.36 (t, J = 7.03 Hz, 1H), 7.12–7.19 (m, 1H), 7.05 (dd, J = 1.76, 8.03 Hz, 1H), 6.90 (d, J = 9.04 Hz, 2H), 6.69 (d, J = 1.76 Hz, 1H), 4.84 (t, J = 5.52 Hz, 1H), 4.65 (d, J = 9.29 Hz, 1H), 4.51 (d, J = 9.54 Hz, 1H), 3.94 (t, J = 5.02 Hz, 2H), 3.83 (d, J = 8.28 Hz, 1H), 3.69 (q, J = 5.10 Hz, 2H), 3.51 (br s, 1H), 1.27 (dd, J = 9.66, 13.93 Hz, 1H), 0.84 (s, 9H), 0.76 (d, J = 13.93 Hz, 1H) ppm; ^{13}C NMR (101 MHz, DMSO-d_6) δ 177.0, 170.8, 156.8, 154.8, 154.3, 143.4, 132.4, 131.5, 129.1, 128.3, 126.3, 126.2, 126.0, 125.0, 124.9, 124.8, 121.4, 120.2, 119.3, 119.1, 114.6, 109.3, 69.7, 65.6, 64.9, 64.6, 59.6, 48.4, 43.2, 40.4, 30.0, 29.7 ppm; HRMS (ES$^+$) m/z calcd for $C_{31}H_{32}Cl_2FN_3O_4$+H [(M+H)$^+$]: 600.1827, found: 600.1824.

4.13. Chiral (2′*S*,3′*R*,4′*S*,5′*R*)-6-chloro-4′-(3-chloro-2-fluoro-phenyl)-2′-(2,2-dimethyl-propyl)-2-oxo-1,2-dihydro-spiro[indole-3,3′-pyrrolidine]-5′-carboxylic acid [4-(2-hydroxy-ethoxy)-2-methoxy-phenyl]-amide (24)

An off white solid (58 mg, 39%). ^{1}H NMR (300 MHz, DMSO-d_6) δ 10.46 (s, 1H), 10.35 (s, 1H), 8.17 (d, J = 8.53 Hz, 1H), 7.69 (d, J = 8.53 Hz, 1H), 7.60 (t, J = 6.84 Hz, 1H), 7.37 (t, J = 6.84 Hz, 1H), 7.16 (t, J = 8.10 Hz, 1H), 7.01 (dd, J = 2.00, 8.10 Hz, 1H), 6.64–6.70 (m, 2H), 6.48 (dd, J = 2.00, 8.91 Hz, 1H), 4.84 (t, J = 5.34 Hz, 1H), 4.56–4.64 (m, 1H), 4.41 (d, J = 9.60 Hz, 1H), 3.96 (t, J = 4.89 Hz, 2H), 3.82 (s, 3H), 3.73–3.81 (m, 1H), 3.61–3.72 (m, 3H), 1.28 (dd, J = 9.60, 13.88 Hz, 1H), 0.90 (s, 9H), 0.75 (d, J = 13.88 Hz, 1H) ppm; ^{13}C NMR (75 MHz, DMSO-d_6) δ 176.9, 170.7, 157.2, 155.1, 153.9, 149.0, 143.4, 132.4, 128.9, 128.4, 126.9, 126.8, 125.8, 125.2, 124.8, 124.7, 121.4, 121.0, 119.3, 119.1, 118.5, 109.2, 104.7, 99.3, 69.8, 66.0, 65.2, 65.0, 59.6, 55.6, 49.1, 42.7, 30.0, 29.6 ppm; HRMS (ES$^+$) m/z Calcd for $C_{32}H_{34}Cl_2FN_3O_5$+H [(M+H)$^+$]: 630.1933, found: 630.1934. $[\alpha]_D^{20} = -28.5°$ (c 0.07, MeOH).

4.14. General procedures for preparation of compounds 25, 26, and 27 from corresponding racemic 4-, 5-, or 7-fluoro intermediate 17 (R^3 = F, R^1 = $CH_2C(CH_3)_3$)

Step (*A*): In a manner similar to the method described in general procedures for compounds **20**–**22** and **4**, the corresponding racemic 4-, 5-, or 7-fluoro carboxylic acid intermediate 17 (R^3 = F, R^1 = $CH_2C(CH_3)_3$, preparation in SI section) (0.33 g, 0.55 mmol), was reacted with diisopropylethylamine (0.29 g, 2.2 mmol), diphenylphosphinic chloride (0.26 g, 1.1 mmol), then reacted with 4-amino-3-methoxy benzonitrile (0.11 g, 0.8 mmol) or 4-amino-benzonitrile (Aldrich) (0.2 g, 1.7 mmol) to give racemic coupled product as a white solid (Yield 0.1 g, 31%).

Step (*B*): To the solution of above racemic coupled product (0.1 g, 0.17 mmol) from (A) in DMSO (5 mL) at 0 °C was added an aqueous solution (30% Aldrich) of H_2O_2 (0.39 g, 3.4 mmol), then aqueous solution (1 N) of NaOH (1.7 mL, 1.7 mmol) was added dropwise. The reaction mixture was stirred at 0 °C for 1 h. The mixture was partitioned between ethyl acetate and saturated aqueous Na_2SO_3 solution. The organic layer was separated, washed with water, brine, dried over $MgSO_4$, and concentrated. The residue was triturated with dichloromethane and hexanes to give the product as a white solid (yield 0.1 g, 97%).

Step (*C*) The above racemic product from (B) (0.11 g) was separated by chiral SFC chromatography (prep OJ, or AD, or OD, 35 °C at 100 bar, eluting with 20–40% methanol in carbon dioxide) to provide pure two enantiomers (>95% ee).

4.15. Chiral (2′*S*,3′*R*,4′*S*,5′*R*)-6-chloro-4′-(3-chloro-2-fluoro-phenyl)-2′-(2,2-dimethyl-propyl)-4-fluoro-2-oxo-1,2-dihydro-spiro[indole-3,3′-pyrrolidine]-5′-carboxylic acid (4-carbamoyl-2-methoxy-phenyl)-amide (25)

A white solid (56 mg, 31%). ^{1}H NMR (400 MHz, DMSO-d_6) δ 10.81 (s, 1H), 10.60 (s, 1H), 8.32 (d, J = 8.28 Hz, 1H), 7.94 (br s, 1H), 7.57–7.65 (m, 3H), 7.51 (dd, J = 1.38, 8.28 Hz, 1H), 7.41 (t, J = 7.03 Hz, 1H), 7.31 (br s, 1H), 7.16–7.24 (m, 1H), 7.00 (dd, J = 2.01, 9.54 Hz, 1H), 6.56 (dd, J = 2.01, 8.53 Hz, 1H), 4.91 (d, J = 8.53 Hz, 1H), 4.69–4.78 (m, 1H), 4.20 (t, J = 10.52 Hz, 1H), 3.91 (s, 3H), 3.79–3.88 (m, 1H), 1.37 (dd, J = 10.52, 13.93 Hz, 1H), 0.91–0.98 (m, 11H), 0.84 (d, J = 13.93 Hz, 1H) ppm; ^{13}C NMR (101 MHz, DMSO-d_6) δ 176.0, 172.0, 167.2, 163.4, 160.9, 156.9, 154.4, 147.5, 145.3, 145.2, 130.4, 130.3, 129.6, 129.4, 129.3, 128.6, 126.2, 126.1, 124.9, 120.4, 119.3, 119.1, 118.1, 109.9, 66.9, 64.6, 60.8, 55.8, 45.3, 43.0, 30.2, 29.5 ppm; HRMS (ES$^+$) m/z calcd for $C_{31}H_{30}Cl_2F_2N_4O_4$+H [(M+H)$^+$]: 631.1685, found: 631.1683.

4.16. Chiral (2′*S*,3′*R*,4′*S*,5′*R*)-6-chloro-4′-(3-chloro-2-fluoro-phenyl)-2′-(2,2-dimethyl-propyl)-5-fluoro-2-oxo-1,2-dihydro-spiro[indole-3,3′-pyrrolidine]-5′-carboxylic acid (4-carbamoyl-phenyl)-amide (26)

An off white solid (43 mg, 29%). ^{1}H NMR (400 MHz, DMSO-d_6) δ 10.47 (s, 1H), 10.21 (s, 1H), 7.91 (d, J = 9.29 Hz, 1H), 7.87 (d, J = 8.78 Hz, 3H), 7.62 (d, J = 8.78 Hz, 2H), 7.55–7.60 (m, 1H), 7.36–7.41 (m, 1H), 7.25 (br s, 1H), 7.17 (t, J = 8.03 Hz, 1H), 6.80 (d, J = 6.27 Hz, 1H), 4.72 (d, J = 8.53 Hz, 1H), 4.57 (d, J = 9.54 Hz, 1H), 3.92 (br s, 1H), 3.45–3.50 (m, 1H), 1.22–1.33 (m, 1H), 0.87 (s, 9H), 0.78 (d, J = 13.74 Hz, 1H) ppm; HRMS (ES$^+$) m/z Calcd for $C_{30}H_{28}Cl_2F_2N_4O_3$+H [(M+H)$^+$]: 601.1580, found: 601.1581.

4.17. Racemic (2′*S*,3′*R*,4′*S*,5′R)-6-chloro-4′-(3-chloro-2-fluoro-phenyl)-2′-(2,2-dimethyl-propyl)-7-fluoro-2-oxo-1,2-dihydro-spiro[indole-3,3′-pyrrolidine]-5′-carboxylic acid (4-carbamoyl-2-methoxy-phenyl)-amide (27)

A light yellow solid (82 mg, 92%). ^{1}H NMR (400 MHz, DMSO-d_6) δ 11.10 (s, 1H), 10.68 (s, 1H), 8.33 (d, J = 8.28 Hz, 1H), 7.93 (br s, 1H), 7.56–7.64 (m, 3H), 7.50 (dd, J = 1.51, 8.28 Hz, 1H), 7.36–7.42 (m, 1H), 7.30 (br s, 1H), 7.14–7.22 (m, 2H), 4.65–4.71 (m, 1H), 4.51 (d, J = 9.29 Hz, 1H), 3.89 (s, 3H), 3.83–3.93 (m, 1H), 3.72–3.80 (m, 1H), 1.30 (dd, J = 9.91, 13.93 Hz, 1H), 0.91 (s, 9H), 0.77 (d, J = 13.93 Hz, 1H) ppm; HRMS (ES$^+$) m/z Calcd for $C_{31}H_{30}Cl_2F_2N_4O_4$+H [(M+H)$^+$]: 631.1685, found: 631.1686.

Acknowledgments

The authors would like to thank Theodore Lambros for SFC purification, Gino Sasso for detailed ^{1}H and NOE NMR analysis of stereochemical assignments, Samir Serrano for high resolution mass spectrometry, Simon Yang, Roche China for optical rotation, and Francisco Talamas for proof reading of the manuscript.

Supplementary data

Supplementary data (the data include syntheses, X-ray crystal data of **5** and **20**, and biological assays) associated with this article can be found, in the online version, at http://dx.doi.org/10.1016/j.bmc.2014.05.072.

References and notes

1. Harris, S. L.; Levine, A. J. *Oncogene* **2005**, *24*, 2899.
2. Michael, D.; Oren, M. *Semin. Cancer Biol.* **2003**, 49.
3. Levine, A. J. *Cell* **1997**, *88*, 323.
4. Vogelstein, B.; Lane, D.; Levine, A. J. *Nature* **2000**, *408*, 307.
5. Wu, X.; Bayle, J. H.; Olson, D.; Levine, A. J. *Gene Dev.* **1993**, *7*, 1126.
6. Hainaut, P.; Hollstein, M. *Adv. Cancer Res.* **2000**, *77*, 81.
7. Vousden, K. H.; Lane, D. P. *Nat. Rev. Mol. Cell Biol.* **2007**, *8*, 275.
8. Bond, G. L.; Hu, W.; Levine, A. J. *Curr. Cancer Drug Targets* **2005**, *5*, 3.
9. Wade, M.; Wang, Y. V.; Wahl, G. M. *Trends Cell Biol.* **2010**, *20*, 299.
10. (a) Vassilev, L. T. *Trends Mol. Med.* **2007**, *13*, 23; (b) Poyurovsky, M. V.; Prives, C. *Gene Dev.* **2006**, *20*, 125; (c) Brown, C. J.; Lain, S.; Verma, C. S.; Fersht, A. R.; Lane, D. P. *Nat. Rev. Cancer* **2009**, *9*, 862; (d) Cheok, C. F.; Verma, C. S.; Baselga, J.; Lane, D. P. *Nat. Rev. Clin. Oncol.* **2011**, *8*, 25.
11. Kussie, P. H.; Gorina, S.; Marechal, V.; Elenbaas, B.; Moreau, J.; Levine, A. J.; Pavletich, N. P. *Science* **1996**, *274*, 948.
12. Vassilev, L. T.; Vu, B. T.; Graves, B.; Carvajal, D.; Podlaski, F.; Filipovic, Z.; Kong, N.; Kammlott, U.; Lukacs, C.; Klein, C.; Fotouhi, N.; Liu, E. A. *Science* **2004**, *303*, 844.
13. (a) Ray Coquard, I.; Blay, J. Y.; Italiano, A.; Le Cesne, A.; Penel, N.; Zhi, J.; Heil, F.; Rueger, R.; Graves, B.; Ding, M.; Geho, D.; Middleton, S. A.; Vassilev, L. T.; Nichols, G. L.; Bui, B. N. *Lancet Oncol.* **2012**, *13*, 1133; (b) Tovar, C.; Graves, B.; Packman, K.; Filipovic, Z.; Higgins, B.; Xia, M.; Tardell, C.; Garrido, R.; Lee, E.; Kolinsky, K.; To, K.-H.; Linn, M.; Podlaski, F.; Wovkulich, P.; Vu, B.; Vassilev, L. T. *Cancer Res.* **2013**, *73*, 2587; (c) Vu, B.; Wovkulich, P.; Pizzolato, G.; Lovey, A.; Ding, Q.; Jiang, N.; Liu, J.-J.; Zhao, C.; Glenn, K.; Wen, Y.; Tovar, C.; Packman, K.; Vassilev, L.; Graves, B. *ACS Med. Chem. Lett.* **2013**, *4*, 466.
14. Ding, Q.; Zhang, Z.; Liu, J.-J.; Jiang, N.; Zhang, J.; Ross, T. M.; Chu, X.-J.; Bartkovitz, D.; Podlaski, F. J.; Janson, C.; Tovar, C.; Filipovic, Z. M.; Higgins, B.; Glenn, K.; Packman, K.; Vassilev, L.; Graves, B. *J. Med. Chem.* **2013**, *56*, 5979.
15. (a) Carry, J.-C.; Garcia-Echeverria, C. *Bioorg. Med. Chem. Lett.* **2013**, *23*, 2480; (b) Sun, D.; Li, Z.; Rew, Y.; Gribble, M.; Bartberger, M. D.; Beck, H. P.; Canon, J.; Chen, A.; Chen, X.; Chow, D.; Deignan, J.; Duquette, J.; Eksterowicz, J.; Fisher, B.; Fox, B. M.; Fu, J.; Gonzalez, A. Z.; Gonzalez-Lopez De Turiso, F.; Houze, J. B.; Huang, X.; Jiang, M.; Jin, L.; Kayser, F.; Liu, J. J.; Lo, M. C.; Long, A. M.; Lucas, B.; McGee, L. R.; McIntosh, J.; Mihalic, J.; Oliner, J. D.; Osgood, T.; Peterson, M. L.; Roveto, P.; Saiki, A. Y.; Shaffer, P.; Toteva, M.; Wang, Y.; Wang, Y. C.; Wortman, S.; Yakowec, P.; Yan, X.; Ye, Q.; Yu, D.; Yu, M.; Zhao, X.; Zhou, J.; Zhu, J.; Olson, S. H.; Medina, J. C. *J. Med. Chem.* **2014**, *57*, 1454.
16. (a) Ding, K.; Lu, Y.; Nikolovska-Coleska, Z.; Qiu, S.; Ding, Y.; Gao, W.; Stuckey, J.; Krajewski, K.; Roller, P. P.; Tomita, Y.; Parrish, D. A.; Deschamps, J. R.; Wang, S. *J. Am. Chem. Soc.* **2005**, *127*, 10130; (b) Ding, K.; Lu, Y.; Nikolovska-Coleska, Z.; Wang, G.; Qiu, S.; Shangary, S.; Gao, W.; Qin, D.; Stuckey, J.; Krajewski, K.; Roller, P. P.; Wang, S. *J. Med. Chem.* **2006**, *49*, 3432; (c) Yu, S.; Qin, D.; Shangary, S.; Chen, J.; Wang, G.; Ding, K.; McEachern, D.; Qiu, S.; Nikolovska-Coleska, Z.; Miller, R.; Kang, S.; Yang, D.; Wang, S. *J. Med. Chem.* **2009**, *52*, 7970.
17. Zhao, Y.; Liu, L.; Sun, W.; Lu, J.; McEachern, D.; Li, X.; Yu, S.; Bernard, D.; Ochsenbein, P.; Ferey, V.; Carry, J.-C.; Deschamps, J. R.; Sun, D.; Wang, S. *J. Am. Chem. Soc.* **2013**, *135*, 7223.
18. Zhao, Y.; Yu, S.; Sun, W.; Liu, L.; Lu, J.; McEachern, D.; Shargary, S.; Bernard, D.; Li, X.; Zhao, T.; Zou, P.; Sun, D.; Wang, S. *J. Med. Chem.* **2013**, *56*, 5553.
19. Bartkovitz, D. J.; Chu, X. -J.; Ding, Q.; Graves, B. J.; Jiang, N.; Zhang, J.; Zhang, Z. PCT Int. Appl. WO 2011 067185, 2011.
20. Luk, K. -C.; So, S. -S.; Zhang, J.; Zhang, Z. PCT Int. Appl. WO 2006136606, 2006.
21. Chen, L.; Ding, Q.; Liu, J. -J.; Yang, S.; Zhang, Z. U.S. Pat. Appl. Publ. US 20080009486, 2008.
22. Liu, J. -J.; Tilley, J. W.; Zhang, Z. U.S. Pat. Appl. Publ. US 20080287421, 2008.
23. Wang, S.; Zhao, Y.; Bernard, D.; Aguilar, A.; Kumar, S. *Top. Med. Chem.* **2012**, *8*, 57.
24. Popowicz, G. M.; Dömling, A.; Holak, T. A. *Angew. Chem., Int. Ed.* **2011**, *50*, 2680.
25. Pfafferott, C.; Oberhammer, H.; Boggs, J. E.; Caminatil, C. W. *J. Am. Chem. Soc.* **1985**, *107*, 2305.
26. (a) De Tar, D.; Luthra, N. P. *J. Am. Chem. Soc.* **1977**, *99*, 1232; (b) Cremer, D.; Pople, J. A. *J. Am. Chem. Soc.* **1975**, *97*, 1354.
27. Koskinenm, A. M.; Helaja, J.; Kumpulainen, E. T.; Koivisto, J.; Mansikkamäki, H.; Rissanen, K. *J. Org. Chem.* **2005**, *70*, 6447.
28. Popowicz, G. M.; Czarna, A.; Wolf, S.; Wang, K.; Wang, W.; Dömling, A.; Holak1, T. A. *Cell Cycle* **2010**, *9*, 1104.
29. Shu, L.; Li, Z.; Gu, C.; Fishlock, D. *Org. Process Res. Dev.* **2013**, *17*, 247.
30. Alemparte, C.; Blay, G.; Jørgensen, K. A. *Org. Lett.* **2005**, *7*, 4569.
31. Grigg, R.; Montgomery, J.; Somasundeam, A. *Tetrahedron* **1992**, *48*, 10431.
32. Cabrera, S.; Arrayás, R. G.; Belén Martín-Matute, A.; Cossío, F. P.; Carretero, J. C. *Tetrahedron* **2007**, *63*, 6587.
33. Awata, A.; Arai, T. *Chem. Eur. J.* **2012**, *18*, 8278.
34. Linke, K.; Mace, P. D.; Smith, C. A.; Vaux, D. L.; Silke, J.; Day, C. L. *Cell Death Differ.* **2008**, *15*, 841.
35. (a) Bernal, F.; Tyler, A. F.; Korsmeyer, S. J.; Walensky, L. D.; Verdine, G. L. *J. Am. Chem. Soc.* **2007**, *129*, 2456; (b) Baek, S.; Kutchukian, P. S.; Verdine, G. L.; Huber, R.; Holak, T. A.; Lee, W. K.; Popowicz, G. M. *J. Am. Chem. Soc.* **2012**, *134*, 103.
36. Zhang, Z.; Chu, X.-J.; Liu, J.-J.; Ding, Q.; Zhang, J.; Bartkovitz, D.; Jiang, N.; Karnach, P.; So, S.-S.; Tovar, C.; Filipovic, Z. M.; Higgins, B.; Glenn, K.; Packman, K.; Vassilev, L.; Graves, B. *ACS. Med. Chem. Lett.* **2014**, *5*, 124.